

A theory of finite deformation magneto-viscoelasticity

Prashant Saxena, Mokarram Hossain, Paul Steinmann
Chair of Applied Mechanics, University of Erlangen-Nuremberg,
Egerlandstrasse 5, 91058 Erlangen, Germany

Abstract

This paper deals with the mathematical modelling of large strain magneto-viscoelastic deformations. Energy dissipation is assumed to occur both due to the mechanical viscoelastic effects as well as the resistance offered by the material to magnetisation. Existence of internal damping mechanisms in the body is considered by decomposing the deformation gradient and the magnetic induction into ‘elastic’ and ‘viscous’ parts. Constitutive laws for material behaviour and evolution equations for the non-equilibrium fields are derived that agree with the laws of thermodynamics. To illustrate the theory the problems of stress relaxation, magnetic field relaxation, time dependent magnetic induction and strain are formulated and solved for a specific form of the constitutive law. The results, that show the effect of several modelling parameters on the deformation and magnetisation process, are illustrated graphically.

1 Introduction

Magnetorheological elastomers (MREs) are materials that change their mechanical behaviour in response to the application of an external magnetic field. These elastomers have received considerable attention in recent years due to their potential uses as variable stiffness actuators for mechanical systems with electronic controls. MREs are particularly useful for their tuneable elastic modulus and a rapid response to the magnetic field, cf. Böse et al.

Corresponding author: Paul Steinmann
Email: paul.steinmann@ltm.uni-erlangen.de
Ph: +49 9131 8528501, Fax: +49 9131 8528503

(2012). A common preparation method is mixing magnetically permeable particles into liquid monomer and letting the mixture to polymerise. Curing, when done in the absence of magnetic field, results in an isotropic material while curing in the presence of a magnetic field causes the particles to align in a particular direction and results in a material with a directional anisotropy. The ferromagnetic particles are usually between 1–5 μm in size and kept between 0–30% by volume of the entire mixture. Such elastomers have been reported to be prepared and analysed by Jolly et al. (1996), Ginder et al. (2002), Varga et al. (2006), Boczkowska and Awietjan (2009), and Böse and Röder (2009).

Mathematical modelling of the coupling of electromagnetic fields in deformable materials has been an area of active research in the past, see, for example, the works of Pao (1978) and Eringen and Maugin (1990). Recently, a new constitutive formulation based on a ‘total’ energy density function has been developed by Dorfmann and Ogden (2003, 2004), wherein the solutions of some boundary value problems were obtained using different energy densities. It has been shown that any one of the magnetic induction vector, magnetic field vector, or the magnetisation vector can be used as an independent variable of the problem and the other two obtained through the constitutive relations. The relevant equations used by them are based on the classic work of Pao (1978) in which the equations of motion for an isotropic non-polar continuum in an electromagnetic field are described by Maxwell’s equations and the mechanical and thermodynamical balance laws. This formulation has been particularly useful in recent years in dealing with problems related to magnetoelasticity and using this, further boundary value problems on nonlinear deformation and wave propagation have been studied by Bustamante et al. (2007), Otténio et al. (2008) and Saxena and Ogden (2011).

The response to an applied magnetic induction is, however, not exactly instantaneous for all materials. On the application of a sudden external magnetic induction, the magnetic field (or equivalently the magnetisation) developed inside the material is not constant. Starting with some initial non-equilibrium value, it gradually approaches equilibrium in some finite time (say t_1) depending on the existing deformation and various material parameters. The synthetically developed magnetoelastic materials are usually polymer based, hence also viscoelastic in nature. Thus there is development of a viscous overstress on deformation or on the application of a body force that vanishes after a time t_2 which is usually different from t_1 above. This time-delay in response is a very important factor to consider while designing electromechanical actuators from magnetorheological elastomers. Thus, these two forms of dissipation – due to mechanical and due to magnetic effects

need to be modelled appropriately. In order to consider the magnetic and mechanical dissipation effects, the previously stated theory of magnetoelasticity by Dorfmann and Ogden (2004) is generalised by combining with the existing theory of mechanical viscoelasticity.

Viscoelastic material modelling can generally be classified into two main classes, i.e. purely phenomenologically-motivated and micromechanical based network models. In some literature, the viscoelastic modelling approach is also divided, on the one hand, due to the nature of the time-dependent part of the stress, on the other hand, due to the nature of the evolution equation. The phenomenological modelling approach can also be distinguished based on the type of internal variables, i.e. stress type internal variables in the form of convolution integrals, cf. Simo (1987), Holzapfel and Simo (1996), Lion (1997), Kaliske and Rothert (1997); and strain-type internal variables that originate from a multiplicative decomposition of the deformation gradient, cf. Reese and Govindjee (1998) and Huber and Tsakmakis (2000). The latter group decomposes the deformation gradient into elastic and inelastic parts where the inelastic part is determined from a differential type flow rule. In both the cases, the total stress is decomposed into a viscosity induced overstress and an equilibrium stress that corresponds to stress response at an infinitely slow rate of deformation or the stress response when the time-dependent viscous effects are completely diminished. Within the setting of the multiplicative decomposition of the deformation gradient, Reese and Govindjee (1998) proposed an evolution law which, when linearized around the thermodynamical equilibrium, yields the finite linear viscoelastic model of Lubliner (1985). Koprowski-Theiss et al. (2011) proposed a nonlinear evolution law, which after being proved to be thermodynamically consistent, has been used in this paper. For the modelling based on stress-type internal variables, the time-dependent overstress part is expressed as an integral over the deformation history, cf., Simo (1987) and Amin et al. (2006).

The second class of viscoelastic material modelling is based on micromechanical theories derived using the underlying molecular structures, see, for example, the works of Bird et al. (1987), Doi and Edwards (1988), Bergström and Boyce (1998) and Miehe and Göktepe (2005). These have been developed over the years to describe the viscous behaviour of molten polymers and physically cross-linked rubber-like materials. The bead-spring model of Bird et al. (1987), the reptation-type tube models of de Gennes (1971) and Doi and Edwards (1988), and the transient network models of Green and Tobolsky (1946) can be mentioned as examples in this area. The theory for transient network models explains the stress relaxation phenomena as a consequence of breakage and reformulation of the polymer cross-links constantly, cf. Green and Tobolsky (1946) and Reese (2003). Reptation-type

tube models are developed for the definition of the motion of a single chain in a polymer gel. The constraints on the free motion of a single chain are qualitatively modelled as a tube-like constraint and the motion of the chain is described as a combination of Brownian motion within and reptational motion along the tube. Recently, a growing interest can be observed to combine these approaches which yield the so-called micromechanically motivated models, see, for example, Linder et al. (2011).

As a first step in the magneto-viscoelastic modelling, we model an isotropic material and take a phenomenological approach based on the multiplicative decomposition of the deformation gradient in line with Lubliner (1985). An additive decomposition of the magnetic induction vector into equilibrium and non-equilibrium parts is proposed to model magnetic dissipation phenomena. The equilibrium part of the energy is taken to be a generalisation of the Mooney–Rivlin elastic model to include magnetic effects, while the non-equilibrium part is a slightly simplified version that looks like a neo-Hookean type magnetoelastic model. Using a Clausius–Duhem form of the second law of thermodynamics, we obtain evolution equations for these physical quantities to be able to perform numerical calculations.

This paper is organised as follows. In Section 2, the theory of nonlinear magneto-viscoelasticity is presented taking into account the case of finite deformation. Starting with the governing Maxwell’s equations and the laws of momentum balance, we show the existence of a total stress tensor of Dorfmann and Ogden (2003). The deformation gradient and the magnetic induction are decomposed into equilibrium and non-equilibrium parts. Using the laws of thermodynamics and a form of the Helmholtz free energy function, constitutive equations are derived along with the conditions to be satisfied by the evolution equations of the non-equilibrium quantities.

In Section 3, for the purpose of obtaining numerical solutions the energy density function and the evolution equations for the non-equilibrium quantities are specialised to specific forms. Several material parameters to model magneto-viscoelastic coupling are introduced in this step. In Section 4, we consider four different types of deformation and magnetisation processes to study the effects of the underlying magnetic induction, deformation, strain rate and magnetic induction rate on the total Cauchy stress and the magnetic field relaxation process. It is observed that changing the newly defined magneto-viscoelastic coupling parameters can affect the magnitude of the overstress, the excess magnetic field and their decay times. Initial deformation can affect the decay time and magnitude of the induced magnetic field. Effects of the deformation, applied magnetic induction and the material parameters on the computed physical quantities (such as stress and magnetic field) are illustrated graphically. Section 5 contains some brief concluding

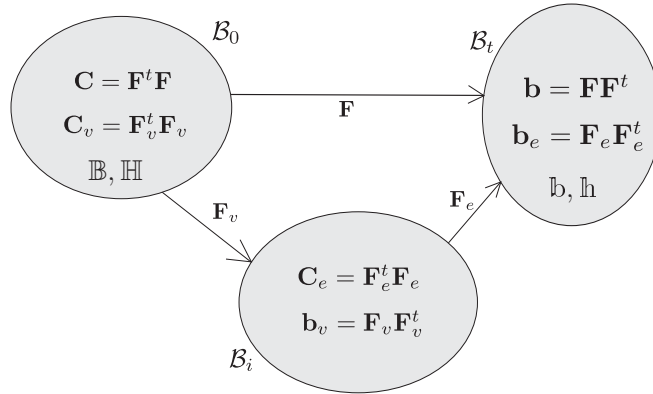


Fig. 1. The material, intermediate, and spatial configurations with the corresponding magnetic vectors and deformation tensors.

remarks.

2 Theory of nonlinear magneto-viscoelasticity

We consider an incompressible magnetoelastic material which, when undeformed and unstressed and in the absence of magnetic fields, occupies the material configuration \mathcal{B}_0 with boundary $\partial\mathcal{B}_0$. It is then subjected to a static deformation due to the combined action of a magnetic field and mechanical surface and body forces. The spatial configuration at time t is denoted by \mathcal{B}_t with a boundary $\partial\mathcal{B}_t$. The two configurations are related by a deformation function χ which maps every point $\mathbf{X} \in \mathcal{B}_0$ to a point $\mathbf{x} = \chi(\mathbf{X}, t) \in \mathcal{B}_t$. The deformation gradient is defined as $\mathbf{F} = \text{Grad } \chi$, where Grad is the gradient operator with respect to \mathbf{X} . Its determinant is given by $J = \det \mathbf{F} \equiv 1$ for the present case of incompressibility.

To take into account mechanical viscous effects, we assume the existence of an intermediate configuration \mathcal{B}_i that is related to \mathcal{B}_t by a purely elastic deformation and is related to \mathcal{B}_0 by a pure viscous motion. The intermediate configuration \mathcal{B}_i is postulated only to model the dissipation effects. This is in parallel to the energy-conserving magnetoelastic deformation from \mathcal{B}_0 to \mathcal{B}_t . Following Lubliner (1985) and Reese and Govindjee (1998), this motivates the decomposition of the deformation gradient into an elastic and a viscous part as

$$\mathbf{F} = \mathbf{F}_e \mathbf{F}_v. \quad (1)$$

For future use we define the right and the left Cauchy–Green strain tensors

as $\mathbf{C} = \mathbf{F}^t \mathbf{F}$ and $\mathbf{b} = \mathbf{F} \mathbf{F}^t$, respectively. Similar quantities corresponding to \mathbf{F}_v and \mathbf{F}_e are defined in $\mathcal{B}_0, \mathcal{B}_i$ and \mathcal{B}_t as shown in Fig. 1.

It is further assumed that the material is electrically non-conducting and there are no electric fields. Let $\boldsymbol{\sigma}$ be the ‘mechanical’ Cauchy stress tensor and $\boldsymbol{\tau}$ the total Cauchy stress tensor (see, for example, Dorfmann and Ogden (2004) for its definition), ρ the mass density, \mathbf{f}_m the mechanical body force per unit mass, \mathbf{a} the acceleration of a point, \mathbb{f} the electromagnetic body force per unit volume, \mathbb{h} the magnetic field vector, \mathbb{b} the magnetic induction vector, and \mathbb{m} the magnetisation vector. The following balance laws need to be satisfied

$$\operatorname{div} \boldsymbol{\sigma} + \mathbb{f} + \rho \mathbf{f}_m = \rho \mathbf{a}, \quad \operatorname{div} \boldsymbol{\tau} + \rho \mathbf{f}_m = \rho \mathbf{a}, \quad \boldsymbol{\tau}^t = \boldsymbol{\tau}, \quad (2)$$

$$\operatorname{curl} \mathbb{h} = \mathbf{0}, \quad \operatorname{div} \mathbb{b} = 0. \quad (3)$$

In Eq. (2), the first two equations are equivalent forms of the balance of linear momentum and the third is the angular momentum balance equation. Eq. (3)₁ is the specialisation of Ampère’s law appropriate to the present situation and Eq. (3)₂ is the statement of impossibility of the existence of magnetic monopoles. Here and henceforth, grad, div, curl denote the standard differential operators in \mathcal{B}_t while Grad, Div, Curl denote the corresponding operators in \mathcal{B}_0 . The three magnetic vectors are connected through the standard relation

$$\mathbb{b} = \mu_0 [\mathbb{h} + \mathbb{m}], \quad (4)$$

μ_0 being the magnetic permeability of vacuum. The connection between $\boldsymbol{\sigma}$ and $\boldsymbol{\tau}$ is

$$\boldsymbol{\tau} = \boldsymbol{\sigma} + \mu_0^{-1} \left[\mathbb{b} \otimes \mathbb{b} - \frac{1}{2} [\mathbb{b} \cdot \mathbb{b}] \mathbf{i} \right] + [\mathbb{m} \cdot \mathbb{b}] \mathbf{i} - \mathbb{b} \otimes \mathbb{m}, \quad (5)$$

where \mathbf{i} is the second order identity tensor in \mathcal{B}_t and we have used the expression for the magnetic body force as $\mathbb{f} = [\operatorname{grad} \mathbb{b}]^t \mathbb{m}$; see, for example, Pao (1978).

The total Piola-Kirchhoff stress and the Lagrangian forms of \mathbb{h}, \mathbb{m} , and \mathbb{b} for an incompressible material ($J = 1$) are defined by

$$\begin{aligned} \mathbf{S} &= \mathbf{F}^{-1} \boldsymbol{\tau} \mathbf{F}^{-t} \\ &= \mathbf{F}^{-1} \boldsymbol{\sigma} \mathbf{F}^{-t} + \mu_0^{-1} \left[\mathbb{B} \otimes \mathbb{B} - \frac{1}{2} [[\mathbf{C}\mathbb{B}] \cdot \mathbb{B}] \mathbf{C}^{-1} \right] + [\mathbb{M} \cdot \mathbb{B}] \mathbf{C}^{-1} - [\mathbb{B} \otimes \mathbb{M}] \mathbf{C}^{-1}, \end{aligned} \quad (6)$$

$$\mathbb{H} = \mathbf{F}^t \mathbb{h}, \quad \mathbb{M} = \mathbf{F}^t \mathbb{m}, \quad \mathbb{B} = \mathbf{F}^{-1} \mathbb{b}. \quad (7)$$

We use the above relations to rewrite the governing equations (2) and (3) in terms of the Lagrangian variables as

$$\text{Div}(\mathbf{S}\mathbf{F}^t) + \rho\mathbf{f}_m = \rho\mathbf{a}, \quad \mathbf{S}^t = \mathbf{S}, \quad \text{Curl } \mathbb{H} = \mathbf{0}, \quad \text{Div } \mathbb{B} = 0, \quad (8)$$

while the relation (4) becomes

$$\mathbf{C}\mathbb{B} = \mu_0 [\mathbb{H} + \mathbb{M}]. \quad (9)$$

In magnetorheological elastomers, in addition to the mechanical viscoelastic effects, we propose that energy dissipation also occurs due to the resistance offered to magnetisation of the material. On the sudden application of a constant magnetic induction, the magnetic field generated inside the material starts from an initial non-equilibrium value and then evolves to approach an equilibrium value. To model these effects, we assume the existence of a dissipation mechanism by including magnetic induction like ‘elastic’ and ‘viscous’ internal variables \mathbb{b}_e and \mathbb{b}_v , respectively. Their Lagrangian counterparts are given by \mathbb{B}_e and \mathbb{B}_v such that

$$\mathbb{b} = \mathbb{b}_e + \mathbb{b}_v, \quad \mathbb{B} = \mathbb{B}_e + \mathbb{B}_v. \quad (10)$$

The above additive decomposition of the magnetic induction is motivated by a similar decoupling into elastic and viscous parts of the deformation in viscoelasticity theory. Since magnetic induction is a vector, an additive decomposition is applied here as opposed to the multiplicative decomposition of the deformation gradient in Eq. (1). The behaviour of the internal variables defined in the above is assumed such that if a constant magnetic induction \mathbb{B} is applied at time $t = 0$, then at that instant $\mathbb{B}_e = \mathbb{B}$ and $\mathbb{B}_v = \mathbf{0}$. As time progress, the magnetic induction is gradually and entirely transferred to \mathbb{B}_v . Thus,

$$\begin{aligned} \mathbb{B}_e &= \mathbb{B}, \quad \mathbb{B}_v = \mathbf{0} \quad \text{at } t = 0, \\ \mathbb{B}_e &\rightarrow \mathbf{0}, \quad \mathbb{B}_v \rightarrow \mathbb{B} \quad \text{as } t \rightarrow \infty. \end{aligned} \quad (11)$$

2.1 Thermodynamics and constitutive modelling

In this section, starting with the laws of thermodynamics, we use the balance equations (2) and (3) to obtain constitutive laws that define the material behaviour. Necessary conditions of energy dissipation associated with the viscous and the magnetic dissipation processes are obtained that need to be satisfied by any magnetoelastic deformation to be thermodynamically admissible.

Balance of energy is written in the local form as (cf. Pao (1978), Dorfmann and Ogden (2003))

$$\rho \frac{d}{dt} \left(U + \frac{1}{2} |\mathbf{v}|^2 \right) + \operatorname{div} \mathbf{Q} = \operatorname{div} (\boldsymbol{\sigma} \mathbf{v}) + [\rho \mathbf{f}_m + \mathbf{f}] \cdot \mathbf{v} + \rho R + w_e, \quad (12)$$

where U and R denote the internal energy and radiant heating per unit mass, \mathbf{Q} is the heat flux, $\boldsymbol{\sigma}$ is the purely mechanical Cauchy stress, \mathbf{f}_m is the mechanical body force (assumed to be zero in the analysis later), and w_e is the electromagnetic power given for the present case as $w_e = -\mathfrak{m} \cdot d\mathfrak{b}/dt$.

Let S be the specific entropy and ϑ be the temperature. On introducing a specific Helmholtz free energy Ψ through

$$\Psi = U - \vartheta S, \quad (13)$$

and using the Clausius–Duhem form of the second law of Thermodynamics

$$\rho \frac{dS}{dt} + \operatorname{div} \left(\frac{\mathbf{Q}}{\vartheta} \right) - \rho \frac{R}{\vartheta} \geq 0, \quad (14)$$

we arrive at the following inequality

$$-\rho \frac{d\Psi}{dt} + \mathbf{F}^{-1} \boldsymbol{\sigma} : \frac{d\mathbf{F}}{dt} - \mathfrak{m} \cdot \frac{d\mathfrak{b}}{dt} \geq 0. \quad (15)$$

The symbol $:$ denotes a double contraction operation between two second order tensors. In the calculations above use has been made of Eq. (2)₁ and the temperature is assumed to be constant.

We now introduce a total energy function similar to the one used by Dorfmann and Ogden (2004)

$$\Omega(\mathbf{F}, \mathbf{C}_v, \mathbb{B}, \mathbb{B}_v) = \rho \Psi(\mathbf{C}, \mathbf{C}_v, \mathbf{F}\mathbb{B}, \mathbf{F}\mathbb{B}_v) + \frac{1}{2\mu_0} \mathbb{B} \cdot [\mathbf{C}\mathbb{B}]. \quad (16)$$

This considers the magnetic induction vector \mathbb{B} as an independent quantity and leaves the magnetic field \mathbb{H} to be determined using a constitutive law. The magnetisation \mathbb{M} , if required, can be obtained using the relation (9).

The above equation, on differentiation with respect to time gives

$$-\rho \frac{d\Psi}{dt} = -\frac{d\Omega}{dt} + \frac{1}{2\mu_0} \mathbb{B} \cdot \left[\frac{d\mathbf{C}}{dt} \mathbb{B} \right] + \frac{1}{\mu_0} [\mathbf{C}\mathbb{B}] \cdot \frac{d\mathbb{B}}{dt}, \quad (17)$$

while using (7), we obtain

$$-\mathfrak{m} \cdot \frac{d\mathfrak{b}}{dt} = -\mathbb{M} \cdot \left[\mathbf{F}^{-1} \frac{d\mathbf{F}}{dt} \mathbb{B} \right] - \mathbb{M} \cdot \frac{d\mathbb{B}}{dt}. \quad (18)$$

Note that the constraint of incompressibility can be expressed as

$$\frac{dJ^2}{dt} = \mathbf{C}^{-1} : \frac{d\mathbf{C}}{dt} = 0. \quad (19)$$

For an incompressible material, $d\mathbf{C}/dt$ is not arbitrary, but the inequality (15) must be satisfied for every $d\mathbf{C}/dt$ governed by the above constraint. Consequently adding a scalar multiple of this zero term and substituting Eqs. (17) and (18) to the inequality (15), a form of the second law of thermodynamics is obtained in terms of the ‘total’ Piola-Kirchhoff stress tensor and the physical quantities defined in their Lagrangian description as

$$-\frac{d\Omega}{dt} + \frac{1}{2} [\mathbf{S} + p\mathbf{C}^{-1}] : \frac{d\mathbf{C}}{dt} + \mathbb{H} \cdot \frac{d\mathbb{B}}{dt} \geq 0, \quad (20)$$

p being a Lagrange multiplier associated with the constraint. It is noted here that one can equivalently use a nominal stress tensor $\mathbf{T} = \mathbf{F}^{-1}\boldsymbol{\tau}$ instead of \mathbf{S} and take \mathbf{F} as an independent variable instead of \mathbf{C} and substitute in (15). This would result in an inequality that yields the constitutive relations used by Dorfmann and Ogden (2004).

Taking partial derivatives of Ω with respect to its arguments and substituting in the inequality above, we get

$$\begin{aligned} \frac{1}{2} \left[\mathbf{S} - 2\frac{\partial\Omega}{\partial\mathbf{C}} + p\mathbf{C}^{-1} \right] : \frac{d\mathbf{C}}{dt} + \left[\mathbb{H} - \frac{\partial\Omega}{\partial\mathbb{B}} \right] \cdot \frac{d\mathbb{B}}{dt} \\ - \frac{\partial\Omega}{\partial\mathbf{C}_v} : \frac{d\mathbf{C}_v}{dt} - \frac{\partial\Omega}{\partial\mathbb{B}_v} \cdot \frac{d\mathbb{B}_v}{dt} \geq 0, \end{aligned} \quad (21)$$

From the arguments of Coleman and Noll (1963), the following constitutive equations are obtained

$$\mathbf{S} = 2\frac{\partial\Omega}{\partial\mathbf{C}} - p\mathbf{C}^{-1}, \quad \mathbb{H} = \frac{\partial\Omega}{\partial\mathbb{B}}, \quad (22)$$

along with the dissipation condition

$$\frac{\partial\Omega}{\partial\mathbf{C}_v} : \frac{d\mathbf{C}_v}{dt} + \frac{\partial\Omega}{\partial\mathbb{B}_v} \cdot \frac{d\mathbb{B}_v}{dt} \leq 0. \quad (23)$$

For the sake of simplicity in the computations later, we further assume that the non-equilibrium magnetic induction \mathbb{B}_v and the non-equilibrium strain tensor \mathbf{C}_v are independent from each other. This reduces the above inequality to the following separate conditions

$$\frac{\partial\Omega}{\partial\mathbf{C}_v} : \frac{d\mathbf{C}_v}{dt} \leq 0, \quad \frac{\partial\Omega}{\partial\mathbb{B}_v} \cdot \frac{d\mathbb{B}_v}{dt} \leq 0, \quad (24)$$

which should be satisfied by any magnetoelastic deformation process to be thermodynamically admissible.

The total energy stored in the body can be split into an equilibrium part associated with the direct deformation from \mathcal{B}_0 to \mathcal{B}_t , and a viscous part due to the internal variable \mathbb{B}_e and the elastic deformation from \mathcal{B}_i to \mathcal{B}_t . This is a slightly general form of the purely mechanical energy decomposition by Reese and Govindjee (1998)

$$\Omega(\mathbf{C}, \mathbf{C}_v, \mathbb{B}, \mathbb{B}_v) = \Omega_e(\mathbf{C}, \mathbb{B}) + \Omega_v(\mathbf{C}, \mathbf{C}_v, \mathbb{B}, \mathbb{B}_v). \quad (25)$$

Here, the viscous part of the energy depends on the viscous parts of the deformation and the magnetic induction. Thus the arguments of Ω_v can be equivalently changed as either one of $\Omega_v(\mathbf{C}, \mathbf{C}_v, \mathbb{B}_e)$, $\Omega_v(\mathbf{C}_e, \mathbb{B}, \mathbb{B}_v)$ or $\Omega_v(\mathbf{C}_e, \mathbb{B}_e)$.

Substituting this form of Ω into the inequalities (24) we obtain the dissipation conditions that should be necessarily met in order to satisfy the second law of thermodynamics

$$\frac{\partial \Omega_v}{\partial \mathbf{C}_v} : \frac{d\mathbf{C}_v}{dt} \leq 0, \quad (26)$$

$$\frac{\partial \Omega_v}{\partial \mathbb{B}_v} \cdot \frac{d\mathbb{B}_v}{dt} \leq 0. \quad (27)$$

It is noted here that the above theory can easily be generalised to include multiple dissipation mechanisms in the body. In the case of M mechanical and N magnetic mechanisms, we may define $\mathbf{F}_e^1, \dots, \mathbf{F}_e^M; \mathbf{F}_v^1, \dots, \mathbf{F}_v^M; \mathbb{B}_e^1, \dots, \mathbb{B}_e^N; \mathbb{B}_v^1, \dots, \mathbb{B}_v^N$ such that

$$\mathbf{F} = \mathbf{F}_e^i \mathbf{F}_v^i, \quad \forall i = 1, \dots, M, \quad (28)$$

$$\mathbb{B} = \mathbb{B}_e^j + \mathbb{B}_v^j, \quad \forall j = 1, \dots, N. \quad (29)$$

The dissipation condition to be satisfied in this general case is

$$\sum_{i=1}^M \frac{\partial \Omega}{\partial \mathbf{C}_v^i} : \frac{d\mathbf{C}_v^i}{dt} + \sum_{j=1}^N \frac{\partial \Omega}{\partial \mathbb{B}_v^j} \cdot \frac{d\mathbb{B}_v^j}{dt} \leq 0. \quad (30)$$

3 Specialised constitutive laws

With a motivation of obtaining numerical solutions to some magneto-viscoelastic deformation problems, we specialise the energy in (25) to specific forms in this section. Evolution equations for \mathbf{C}_v and \mathbb{B}_v are also derived that satisfy the thermodynamic constraints (26) and (27).

3.1 Energy functions

The material is assumed to be isotropic following which the equilibrium part of the energy density function is considered to be a generalisation of the classical Mooney–Rivlin function to magnetoelasticity of the form

$$\Omega_e = \frac{\mu_e}{4} \left[1 + \alpha_e \tanh \left(\frac{I_4}{m_e} \right) \right] \left[[1 + n] [I_1 - 3] + [1 - n] [I_2 - 3] \right] + qI_4 + rI_6, \quad (31)$$

where I_1, I_2, I_4 and I_6 are the standard scalar invariants in magnetoelasticity (see, for example, Dorfmann and Ogden (2004)) defined as

$$I_1 = \mathbf{C} : \mathbf{I}, \quad I_2 = \frac{1}{2} [I_1^2 - \mathbf{C}^2 : \mathbf{I}], \quad I_4 = [\mathbb{B} \otimes \mathbb{B}] : \mathbf{I}, \\ I_6 = [[\mathbf{CB}] \otimes [\mathbf{CB}]] : \mathbf{I}, \quad (32)$$

\mathbf{I} being the second order identity tensor in \mathcal{B}_0 .

This is a slight generalisation of a Mooney–Rivlin type magnetoelastic energy function proposed by Otténio et al. (2008). Here μ_e is the shear modulus of the material in the absence of a magnetic field and n is a dimensionless parameter restricted to the range $-1 \leq n \leq 1$, as for the classical Mooney–Rivlin model. The term $[1 + \alpha_e \tanh(I_4/m_e)]$ corresponds to an increase in the stiffness due to magnetisation and the phenomenon of magnetic saturation after a critical value of magnetisation. The parameter m_e is required for the purpose of non-dimensionalisation while α_e is a dimensionless positive parameter for scaling. The magnetoelastic coupling parameters q and r have the dimensions of μ_0^{-1} . For $\alpha_e = q = r = 0$, this simplifies to the classical Mooney–Rivlin elastic energy density function widely used to model elastomers.

Let the natural basis vectors in \mathcal{B}_0 be identified with a set of covariant basis vectors $\{\mathbf{G}_\alpha\}$ and its dual basis with a set of contravariant basis vectors $\{\mathbf{G}^\alpha\}$, $\alpha \in \{1, 2, 3\}$. Similarly defining $\{\mathbf{g}_\alpha\}$ and $\{\mathbf{g}^\alpha\}$ for \mathcal{B}_t and $\{\bar{\mathbf{g}}_\alpha\}$ and $\{\bar{\mathbf{g}}^\alpha\}$ for \mathcal{B}_i , we obtain the following forms for the deformation gradient and the right Cauchy–Green strain tensors

$$\mathbf{F} = \mathbf{g}_\alpha \otimes \mathbf{G}^\alpha, \quad \mathbf{C} = [\mathbf{g}_\alpha \cdot \mathbf{g}_\beta] \mathbf{G}^\alpha \otimes \mathbf{G}^\beta, \quad \mathbf{C}_v = [\bar{\mathbf{g}}_\alpha \cdot \bar{\mathbf{g}}_\beta] \mathbf{G}^\alpha \otimes \mathbf{G}^\beta. \quad (33)$$

If a vector \mathbb{B} is written in the natural covariant basis as $\mathbb{B} = B^\alpha \mathbf{G}_\alpha$, then $\mathbf{CB} = B^\beta [\mathbf{g}_\alpha \cdot \mathbf{g}_\beta] \mathbf{G}^\alpha$. Thus the identity tensor used for double contraction in $(32)_{1,4}$ needs to have a covariant set of basis vectors while that used in $(32)_3$ requires a contravariant basis.

To obtain the non-equilibrium part of the energy density function, we consider a simplification of the Mooney–Rivlin type energy in (31) by taking $\alpha_e = 0$ and $n = 1$. Since the non-equilibrium part of energy should depend only on the elastic parts of the deformation gradient and the magnetic induction as assumed earlier, we require I_1 in (32)₁ to obtain the value $\mathbf{C}_e : \mathbf{I}$. This is equivalent to the expression $\mathbf{C} : \mathbf{C}_v^{-1}$ on using Eq. (1). Hence to obtain the non-equilibrium energy, instead of a double contraction with the identity tensor to obtain the invariants in (32), we do so by the contravariant tensor \mathbf{C}_v and the covariant tensor \mathbf{C}_v^{-1} as appropriate and replace the Lagrangian vector \mathbb{B} by \mathbb{B}_e . The energy function thus obtained is similar to a generalisation of a neo-Hookean type energy to include magnetic effects

$$\begin{aligned} \Omega_v(\mathbf{C}, \mathbf{C}_v, \mathbb{B}, \mathbb{B}_v) = & \frac{\mu_v}{2} [\mathbf{C} : \mathbf{C}_v^{-1} - 3] + q_v [(\mathbb{B} - \mathbb{B}_v) \otimes (\mathbb{B} - \mathbb{B}_v)] : \mathbf{C}_v \\ & + r_v [(\mathbf{C} [\mathbb{B} - \mathbb{B}_v]) \otimes (\mathbf{C} [\mathbb{B} - \mathbb{B}_v])] : \mathbf{C}_v^{-1}. \end{aligned} \quad (34)$$

The magneto-viscoelastic coupling parameters q_v and r_v here are similar to q and r used in the definition of Ω_e and we have used the relation $\mathbb{B}_e = \mathbb{B} - \mathbb{B}_v$.

A strong coupling between the mechanical viscous measure \mathbf{C}_v and the magnetic non-equilibrium quantity \mathbb{B}_v is noted here. For the sake of simplicity of our calculations and in the absence of any experimental data, we simplify the above expression by assuming that the magnetic non-equilibrium effects are coupled only with the total deformation \mathbf{C} and not with its viscous component \mathbf{C}_v . This assumption was also used earlier to arrive at the dissipation conditions (24). Thus, by replacing \mathbf{C}_v with \mathbf{I} in (34), a simpler form of the non-equilibrium energy is obtained as

$$\begin{aligned} \Omega_v(\mathbf{C}, \mathbf{C}_v, \mathbb{B}, \mathbb{B}_v) = & \frac{\mu_v}{2} [\mathbf{C}_v^{-1} : \mathbf{C} - 3] + q_v [(\mathbb{B} - \mathbb{B}_v) \otimes (\mathbb{B} - \mathbb{B}_v)] : \mathbf{I} \\ & + r_v [(\mathbf{C} [\mathbb{B} - \mathbb{B}_v]) \otimes (\mathbf{C} [\mathbb{B} - \mathbb{B}_v])] : \mathbf{I}. \end{aligned} \quad (35)$$

3.2 Evolution equations

In order to completely define the magneto-viscoelastic behaviour of a solid material, along with the balance laws and the energy density functions defined in the previous sub-section, we also require evolution laws for the ‘viscous’ quantities \mathbb{B}_v and \mathbf{C}_v . These are postulated such that the laws of thermodynamics are satisfied at every instant and \mathbb{B}_v and \mathbf{C}_v stop evolving when the system reaches an equilibrium state.

For the non-equilibrium part of the magnetic induction we consider the following evolution equation such that the left side of inequality (27) becomes a negative semi-definite quadratic form, automatically satisfying the

thermodynamic constraint. Thus,

$$\begin{aligned}\frac{d\mathbb{B}_v}{dt} &= -\frac{\mu_0}{T_m} \frac{\partial \Omega_v}{\partial \mathbb{B}_v}, \\ &= \frac{2\mu_0}{T_m} [q_v \mathbf{I} + r_v \mathbf{C}^2] [\mathbb{B} - \mathbb{B}_v].\end{aligned}\quad (36)$$

For the mechanical viscous strain tensor, we use the evolution equation as proposed by Koprowski-Theiss et al. (2011)

$$\frac{d\mathbf{C}_v}{dt} = \frac{1}{T_v} \left[\mathbf{C} - \frac{1}{3} [\mathbf{C} : \mathbf{C}_v^{-1}] \mathbf{C}_v \right]. \quad (37)$$

In the equations above, T_v is the specific relaxation time for the viscoelastic component of the dissipation mechanism while T_m is the specific relaxation time for its magnetic component. Typically T_v is of the order of some minutes or even upto a few hours while T_m is of the order of a few seconds or some milliseconds.

It now remains to prove that the evolution equation (37) is thermodynamically consistent with the energy density function (35), i.e. they satisfy the constraint (26).

Consider a fourth order projection tensor defined as

$$\mathbb{I}_{\mathbf{C}_v}^{\text{dev}} = \mathbb{I} - \frac{1}{3} \mathbf{C}_v \otimes \mathbf{C}_v^{-1}, \quad (38)$$

where \mathbb{I} is the fourth order symmetric identity tensor given in component form as

$$[\mathbb{I}]_{ijkl} = \frac{1}{2} (\delta_{ik} \delta_{jl} + \delta_{il} \delta_{jk}), \quad (39)$$

δ_{ij} being the Kronecker-Delta. On a double contraction of this tensor $\mathbb{I}_{\mathbf{C}_v}^{\text{dev}}$ with \mathbf{C} , a multiple of the right side of the evolution law (37) is obtained. Thus,

$$\frac{1}{T_v} \mathbb{I}_{\mathbf{C}_v}^{\text{dev}} : \mathbf{C} = \frac{d\mathbf{C}_v}{dt}. \quad (40)$$

From Eq. (35), we obtain

$$\frac{\partial \Omega_v}{\partial \mathbf{C}_v} = -\frac{\mu_v}{2} \mathbf{C}_v^{-1} \mathbf{C} \mathbf{C}_v^{-1} = \frac{\mu_v}{2} \mathbf{C} : \mathbb{I}_{\mathbf{C}_v^{-1}}, \quad (41)$$

where we have used the negative-definite fourth order projection tensor $\mathbb{I}_{\mathbf{C}_v^{-1}}$ which when expanded in component form, gives

$$[\mathbb{I}_{\mathbf{C}_v^{-1}}]_{ijkl} = -\frac{1}{2} \left[[\mathbf{C}_v^{-1}]_{ik} [\mathbf{C}_v^{-1}]_{jl} + [\mathbf{C}_v^{-1}]_{il} [\mathbf{C}_v^{-1}]_{jk} \right]. \quad (42)$$

Consider the following operation

$$\frac{\partial \Omega_v}{\partial \mathbf{C}_v} : \frac{d\mathbf{C}_v}{dt} = \frac{\mu_v}{2T_v} [\mathbf{C} : \mathbb{I}_{\mathbf{C}_v^{-1}}] : [\mathbb{I}_{\mathbf{C}_v}^{\text{dev}} : \mathbf{C}]. \quad (43)$$

Since the tensor $\mathbb{I}_{\mathbf{C}_v}^{\text{dev}}$ is idempotent, the above expression can be rewritten as

$$\frac{\partial \Omega_v}{\partial \mathbf{C}_v} : \frac{d\mathbf{C}_v}{dt} = \frac{\mu_v}{2T_v} [\mathbf{C} : \mathbb{I}_{\mathbf{C}_v^{-1}}] : \mathbb{I}_{\mathbf{C}_v}^{\text{dev}} : [\mathbb{I}_{\mathbf{C}_v}^{\text{dev}} : \mathbf{C}], \quad (44)$$

$$= \frac{\mu_v}{2T_v} [\mathbb{I}_{\mathbf{C}_v}^{\text{dev}} : \mathbf{C}] : \mathbb{I}_{\mathbf{C}_v^{-1}} : [\mathbb{I}_{\mathbf{C}_v}^{\text{dev}} : \mathbf{C}] \leq 0. \quad (45)$$

The above inequality holds since $\mathbb{I}_{\mathbf{C}_v^{-1}}$ is negative definite. This is the statement of the dissipation condition (26), hence the evolution equation (37) is thermodynamically consistent with the energy density function (35).

3.3 Stress and magnetic field calculations

For the energy functions defined in Eqs. (31) and (35), the Piola–Kirchhoff stress is given as

$$\mathbf{S} = 2 \frac{\partial \Omega_e}{\partial \mathbf{C}} + 2 \frac{\partial \Omega_v}{\partial \mathbf{C}} - p \mathbf{C}^{-1} = \mathbf{S}_e + \mathbf{S}_v - p \mathbf{C}^{-1}, \quad (46)$$

where

$$\begin{aligned} \mathbf{S}_e = \frac{\mu_e}{2} \left[1 + \alpha_e \tanh \left(\frac{I_4}{m_e} \right) \right] & \left[[1 + n] \mathbf{I} + [1 - n] [I_1 \mathbf{I} - \mathbf{C}] \right] \\ & + 2r \mathbb{B} \otimes [\mathbf{C} \mathbb{B}] + 2r [\mathbf{C} \mathbb{B}] \otimes \mathbb{B}, \end{aligned} \quad (47)$$

and

$$\mathbf{S}_v = \mu_v \mathbf{C}_v^{-1} + 2r_v \mathbb{B}_e \otimes [\mathbf{C} \mathbb{B}_e] + 2r_v [\mathbf{C} \mathbb{B}_e] \otimes \mathbb{B}_e. \quad (48)$$

The Lagrangian magnetic field \mathbb{H} is given as

$$\mathbb{H} = \frac{\partial \Omega_e}{\partial \mathbb{B}} + \frac{\partial \Omega_v}{\partial \mathbb{B}} = \mathbb{H}_e + \mathbb{H}_v, \quad (49)$$

where

$$\begin{aligned} \mathbb{H}_e = \frac{\mu_e}{2m_e} \left[1 - \alpha_e \tanh^2 \left(\frac{I_4}{m_e} \right) \right] & \left[[1 + n] [I_1 - 3] + [1 - n] [I_2 - 3] \right] \mathbb{B} \\ & + 2q \mathbb{B} + 2r \mathbf{C}^2 \mathbb{B}, \end{aligned} \quad (50)$$

and

$$\mathbb{H}_v = 2q_v \mathbb{B}_e + 2r_v \mathbf{C} \mathbb{B}_e. \quad (51)$$

The ‘viscous’ or non-equilibrium magnetic field defined above tends to zero at equilibrium when $\mathbb{B}_e \rightarrow \mathbf{0}$. Eulerian expressions for the equilibrium values of the total Cauchy stress $\boldsymbol{\tau}$ and the magnetic field \mathbf{h} can be written using Eqs. (47) and (50) as

$$\boldsymbol{\tau}_e = \frac{\mu_e}{2} \left[1 + \alpha_e \tanh \left(\frac{I_4}{m_e} \right) \right] \left[[1 + n] \mathbf{b} + [1 - n] [I_1 \mathbf{b} - \mathbf{b}^2] \right] + 2r \mathbf{b} \otimes [\mathbf{b}\mathbf{b}] + 2r [\mathbf{b}\mathbf{b}] \otimes \mathbf{b}, \quad (52)$$

$$\mathbf{h}_e = \frac{\mu_e}{2m_e} \left[1 - \alpha_e \tanh^2 \left(\frac{I_4}{m_e} \right) \right] \left[[1 + n] [I_1 - 3] + [1 - n] [I_2 - 3] \right] \mathbf{b}^{-1} \mathbf{b} + 2q \mathbf{b}^{-1} \mathbf{b} + 2r \mathbf{b}\mathbf{b}. \quad (53)$$

In the case of no deformation ($\mathbf{b} = \mathbf{i}$), if $r = 0$, then the total equilibrium stress in Eq. (52) is unaffected by the magnetic induction and if $q = r = 0$ then the equilibrium magnetic field in Eq. (53) is unaffected by the underlying deformation. The coupling caused by the parameters q and r between deformation and magnetic field is inverse to each other. The former causes a directly proportional relation of \mathbf{b}^{-1} to \mathbf{h}_e while the latter links \mathbf{b} to \mathbf{h}_e . Similarly q_v and r_v are required for including these two-way coupling effects for the non-equilibrium quantities.

For the case of no deformation of an isotropic material, the magnetic field should be in the direction of the applied magnetic induction and be directly proportional to the latter. From Eq. (53), this imposes the constraint

$$q + r > 0. \quad (54)$$

If $r > 0$, the material stiffens in the direction of the applied magnetic induction while if $\alpha_e > 0$, the total stiffness of the material increases isotropically. Both these effects have been observed to be the case in many MREs, see, for example, the results of Jolly et al. (1996) and Varga et al. (2006). However, this need not necessarily be true in general for all magnetoelastic materials and r can have negative values. In this situation and the case of a material with weak magnetoelastic coupling, i.e. very small values of r ; we require $q > 0$ to satisfy the constraint (54).

4 Numerical examples

In this section, we model four different types of experiments and obtain the corresponding solutions numerically. The following numerical values of the

material parameters are used unless otherwise stated to have a different value for individual computations

$$\begin{aligned} \mu_0 &= 4\pi \times 10^{-7} \text{ N/A}^2, & \mu_e &= 2.6 \times 10^5 \text{ N/m}^2, & \mu_v &= 5 \times 10^5 \text{ N/m}^2, \\ \alpha_e &= 0.3, & m_e &= 1 \text{ T}^2, & n &= 0.3, & q = r = r_v &= 1/\mu_0, & q_v &= 5/\mu_0. \end{aligned} \quad (55)$$

The value of μ_e is taken to be the value of shear modulus at zero magnetic field for an elastomer filled with 10% by volume of iron particles, cf. Jolly et al. (1996). Values of n, q and r are what have been used by Otténio et al. (2008) and Saxena and Ogden (2011). Values of $\mu_v, \alpha_e, q_v, r_v$ are within reasonable physical assumptions and we analyse the dependence of our solutions on the values of these parameters.

For computations in the following subsections, the equations derived earlier are specialised to a uniaxial deformation and magnetisation in cartesian coordinates. The time-integration is performed using a standard solver `ode45` from Matlab that employs an explicit Runge–Kutta scheme, cf. Shampine and Reichelt (1997).

4.1 Magnetic induction with no deformation

With a motivation to isolate and understand the effects of the applied magnetic induction on the magneto-viscoelastic deformation process, we consider no deformation in this first case. Consider an experiment with the sample held fixed at zero deformation ($\lambda_1 = \lambda_2 = \lambda_3 = 1$) and a sudden but constant magnetic induction applied at time $t = 0$. This results in the generation of a viscous overstress and a temporary increment in the magnetic field, both of which settle down to equilibrium values with time. Variations of the total magnetic field h_1 (component of \mathbf{h} in the x_1 direction) and the total Cauchy stress τ_{11} with time are plotted in Figs. 2–4 for the following values of the magnetic induction.

$$\mathbb{B}_2 = \mathbb{B}_3 = 0, \quad \mathbb{B}_1 = \begin{cases} 0, & \text{for } t < 0, \\ 0.1 \text{ T}, & \text{for } t \geq 0. \end{cases} \quad (56)$$

We study the dependence of the magneto-viscoelastic coupling parameters q_v and r_v , and the applied magnetic induction \mathbb{B}_1 on the relaxation of magnetic field and total Cauchy stress.

It is seen from Fig. 2a that a large value of q_v causes a high initial magnetic field but the decay to equilibrium value is also faster when q_v is high. In the case of the total Cauchy stress, as seen from Fig. 2b, q_v has no effect on the initial viscous overstress but a large q_v also causes the stress to decay

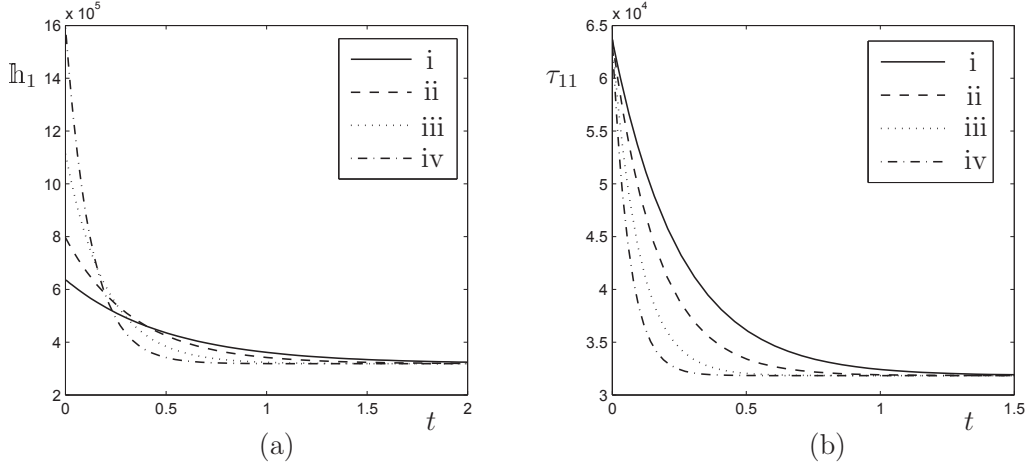


Fig. 2. Variation of **(a)** the total magnetic field h_1 (A/m) and **(b)** the principal total Cauchy stress τ_{11} (N/m²) with time t (s) for no deformation in the presence of a step magnetic induction $B_1 = 0.1$ T. Four curves correspond to different values of q_v (i) $q_v = 1/\mu_0$, (ii) $q_v = 2/\mu_0$, (iii) $q_v = 4/\mu_0$, (iv) $q_v = 7/\mu_0$.

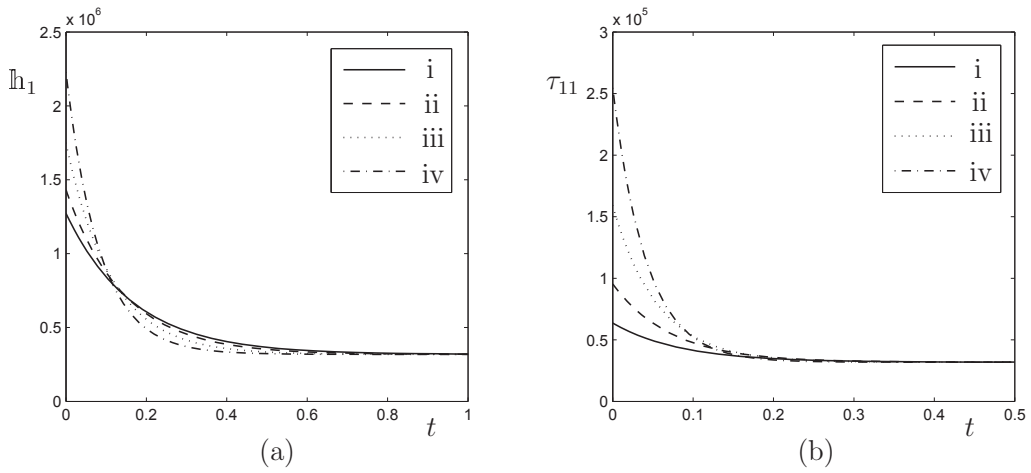


Fig. 3. Variation of **(a)** the total magnetic field h_1 (A/m) and **(b)** the principal total Cauchy stress τ_{11} (N/m²) with time t (s) for no deformation in the presence of a step magnetic induction $B_1 = 0.1$ T. Four curves correspond to different values of r_v (i) $r_v = 1/\mu_0$, (ii) $r_v = 2/\mu_0$, (iii) $r_v = 4/\mu_0$, (iv) $r_v = 7/\mu_0$.

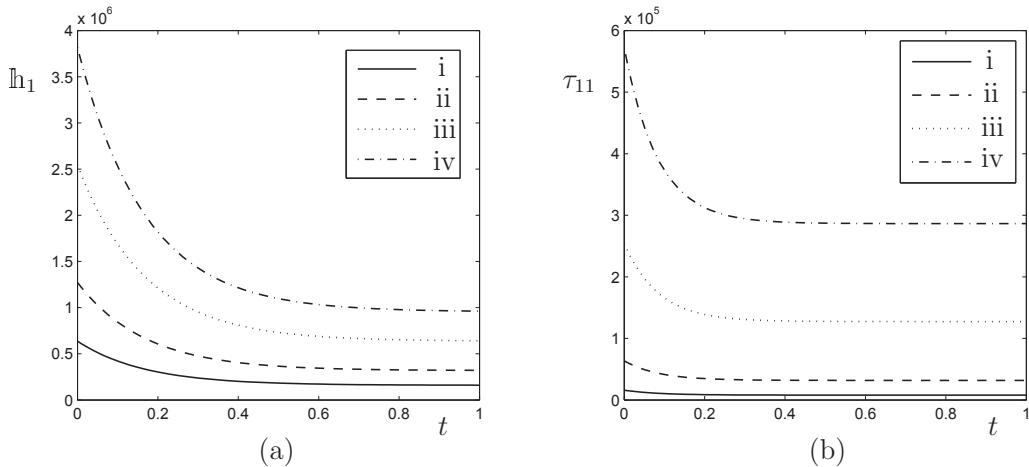


Fig. 4. Variation of **(a)** the total magnetic field h_1 (A/m) and **(b)** the principal total Cauchy stress τ_{11} (N/m²) with time t (s) for different values of the magnetic induction \mathbb{B}_1 (i) $\mathbb{B}_1 = 0.05$ T, (ii) $\mathbb{B}_1 = 0.1$ T, (iii) $\mathbb{B}_1 = 0.2$ T, (iv) $\mathbb{B}_1 = 0.3$ T.

faster and reach the equilibrium value. This is expected since the expression for \mathbf{S}_v in Eq. (48) does not contain q_v explicitly but the dependence comes through the evolution equation (36). The parameter r_v has a similar effect on the magnetic field as does q_v but different in the case of the total Cauchy stress. As observed from Fig. 3, a large value of r_v causes a higher initial stress and a faster decay of the same to equilibrium. The dependence of the relaxation processes on the applied magnetic induction is shown in Fig. 4. It is seen that the equilibrium values for all curves are different in this case since they depend on the value of applied magnetic induction. As expected from Eqs. (52) and (53) a higher magnetic induction causes a larger magnetic field and a larger stress. It is also observed that the higher the magnetic induction, the longer it takes for both the magnetic field and the stress to relax and reach equilibrium.

4.2 Magnetic induction with a uniaxial deformation

In this case, we specify a deformation and a magnetic induction in the x_1 direction while allowing the material to move freely in x_2 and x_3 directions. The stretch λ_1 and the magnetic induction \mathbb{B}_1 are applied at time $t = 0$ and then the material is allowed to relax and reach an equilibrium state. Variation of the magnetic field and the total Cauchy stress with time are

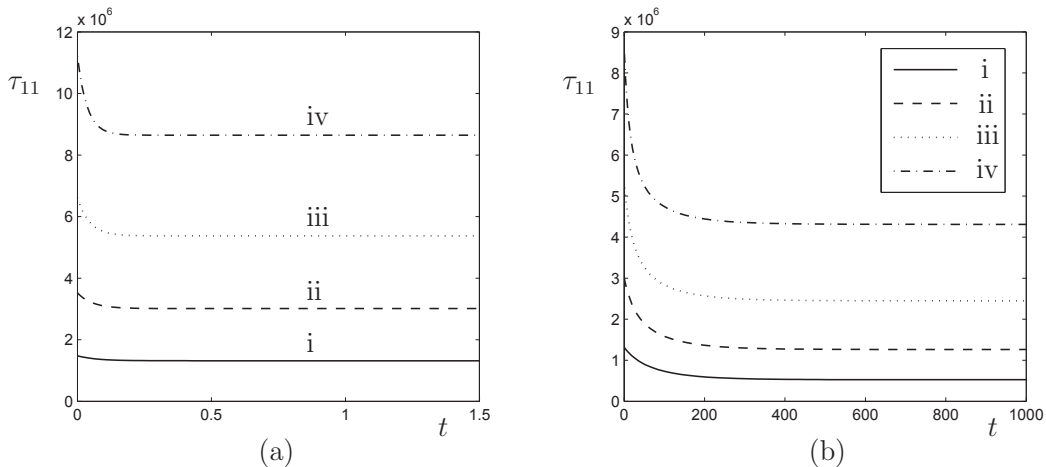


Fig. 5. Uniaxial stretch in x_1 direction, $\mathbb{B}_1 = 0.1$ T. Variation of principal total Cauchy stress τ_{11} (N/m^2) vs time t (s) for different values of the stretch λ_1 . **(a)** small time scale **(b)** large time scale. (i) $\lambda_1 = 1.5$, (ii) $\lambda_1 = 2$, (iii) $\lambda_1 = 3$, (iv) $\lambda_1 = 4$.

plotted in Figs. 5 and 6 for the values

$$T_v = 100 \text{ s}, \quad \mathbb{B}_1 = 0.1 \text{ T}, \quad \lambda_1 = 1.5, \quad (57)$$

unless otherwise stated to be different for individual problems.

It is observed from Fig. 5 that two different relaxations over different time scales occur in the total Cauchy stress τ_{11} – one corresponding to the evolution of \mathbb{B}_v and other corresponding to that of \mathbf{C}_v . The decay for small time scale (upto 1.5 seconds) to reach an equilibrium value is shown in Fig. 5a while that for a longer time scale (upto 1000 seconds) is shown in Fig. 5b. The four curves correspond to four different values of the initial stretch. It should be noted that the end point of a curve in Fig. 5a is the same as the starting point of the corresponding curve in Fig. 5b. A higher stretch causes an increase in the equilibrium value of the magnetic field in Fig. 6a and also causes a faster relaxation to equilibrium value. As expected from the existing results of pure mechanical viscoelasticity, cf. Hossain et al. (2012), a higher stretch leads to a larger value of stress in Fig. 5 and a smaller value of T_v causes stress to relax faster in Fig. 6b.

4.3 Time dependent deformation

We now study the effects of the magneto-viscoelastic coupling on a dynamic deformation of the material. In this case, calculations are performed corre-

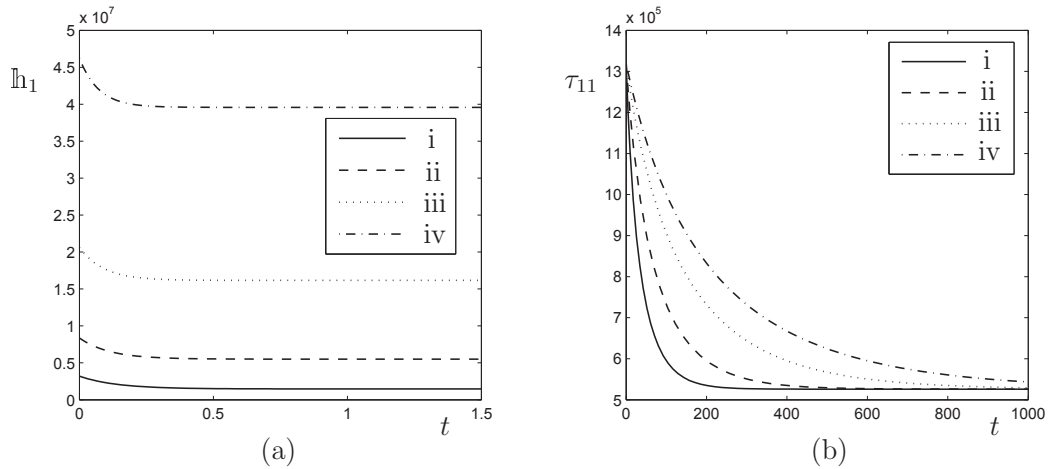


Fig. 6. Uniaxial stretch in x_1 direction, $\mathbb{B}_1 = 0.1$ T. Variation of **(a)** total magnetic field \mathbb{h}_1 (A/m) vs time t (s) for different values of the stretch λ_1 . **(b)** large time scale. (i) $\lambda_1 = 1.5$, (ii) $\lambda_1 = 2$, (iii) $\lambda_1 = 3$, (iv) $\lambda_1 = 4$; **(b)** principal total Cauchy stress τ_{11} (N/m²) vs time t (s) for different values of parameter T_v (i) $T_v = 50$ s, (ii) $T_v = 100$ s, (iii) $T_v = 200$ s, (iv) $T_v = 300$ s.

sponding to an experiment where a magnetic induction is applied at time $t = 0$ and the material is stretched with a constant rate in the x_1 direction. On reaching $\lambda_1 = 3$, stretch is reduced at the same rate until a condition of zero stress or zero deformation (whichever earlier) is reached. Effects on the total Cauchy stress and the total magnetic field of the applied magnetic induction, the rate of stretch, and the parameters q_v and r_v is analysed in Figs. 7–9. The following values of the magnetic induction and the stretch rate are used

$$\mathbb{B}_1 = 0.2 \text{ T}, \quad \dot{\lambda}_1 = \pm 0.01 \text{ s}^{-1}, \quad (58)$$

unless otherwise stated to be different for individual calculations.

It is seen from Fig. 7a that the starting points of all four curves are different corresponding to the stress induced due to the applied magnetic induction. The stress first increases with time (due to an increasing λ_1) and then falls with a decreasing λ_1 following a different path than earlier. A higher magnetic induction leads to larger value of the peak stress reached during the process. Similar curves for different values of the stretch rates are shown in Fig. 7b. A larger value of stretch rate causes a larger peak value of stress since the material gets less time to relax as observed for the purely mechanical viscoelastic case by Lion (1997) and Amin et al. (2006).

Similar variation of the magnetic field \mathbb{h}_1 with the stretch λ_1 can be

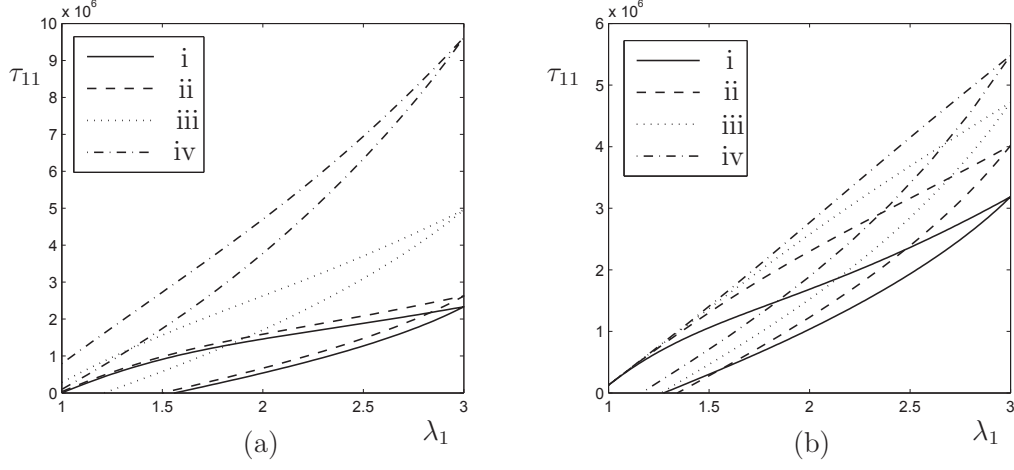


Fig. 7. Principal total Cauchy stress τ_{11} (N/m^2) vs stretch λ_1 . **(a)** Different values of the underlying magnetic induction (i) $\mathbb{B}_1 = 0$, (ii) $\mathbb{B}_1 = 0.1$ T, (iii) $\mathbb{B}_1 = 0.3$ T, (iv) $\mathbb{B}_1 = 0.5$ T. **(b)** Different values of the stretch rate (i) $\dot{\lambda}_1 = \pm 0.005$ s $^{-1}$, (ii) $\dot{\lambda}_1 = \pm 0.02$ s $^{-1}$, (iii) $\dot{\lambda}_1 = \pm 0.04$ s $^{-1}$, (iv) $\dot{\lambda}_1 = \pm 0.08$ s $^{-1}$.

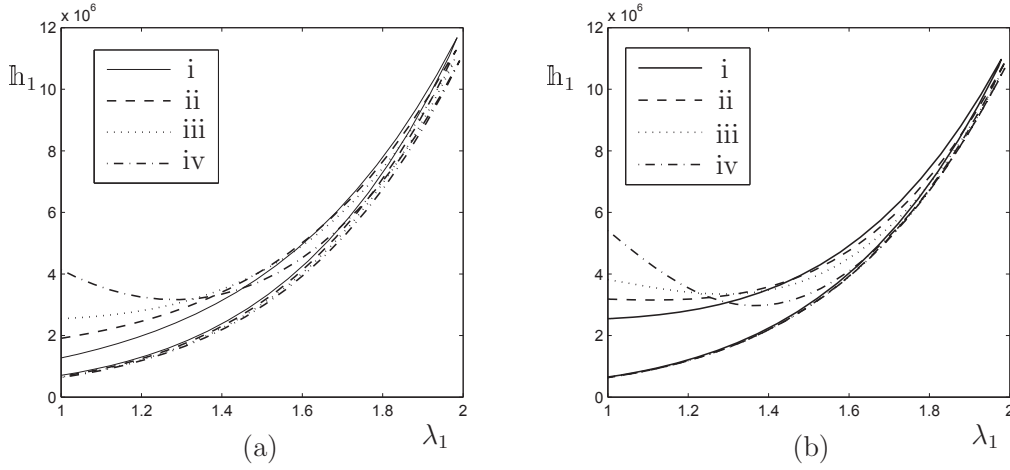


Fig. 8. Total magnetic field h_1 (A/m) vs stretch λ_1 at a stretch rate $\dot{\lambda}_1 = \pm 3$ s $^{-1}$. **(a)** Different values of the parameter q_v (i) $q_v = 1/\mu_0$, (ii) $q_v = 3/\mu_0$, (iii) $q_v = 5/\mu_0$, (iv) $q_v = 10/\mu_0$; **(b)** Different values of the parameter r_v (i) $r_v = 1/\mu_0$, (ii) $r_v = 3/\mu_0$, (iii) $r_v = 5/\mu_0$, (iv) $r_v = 10/\mu_0$.

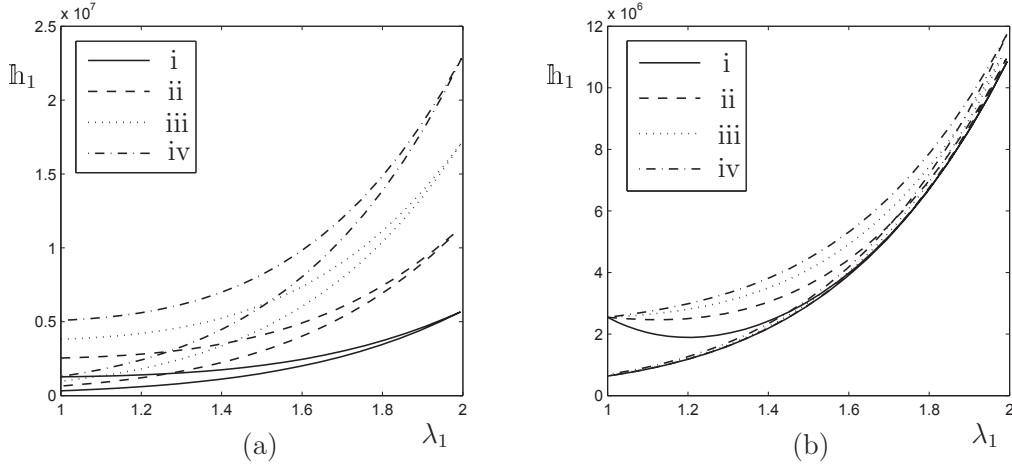


Fig. 9. Total magnetic field h_1 (A/m) vs stretch λ_1 . **(a)** Different values of the magnetic induction \mathbb{B}_1 at a stretch rate $\dot{\lambda}_1 = \pm 3 \text{ s}^{-1}$ (i) $\mathbb{B}_1 = 0.1 \text{ T}$, (ii) $\mathbb{B}_1 = 0.2 \text{ T}$, (iii) $\mathbb{B}_1 = 0.3 \text{ T}$, (iv) $\mathbb{B}_1 = 0.4 \text{ T}$; **(b)** Different values of the stretch rate $\dot{\lambda}_1$ (i) $\dot{\lambda}_1 = 1 \text{ s}^{-1}$, (ii) $\dot{\lambda}_1 = 2 \text{ s}^{-1}$, (iii) $\dot{\lambda}_1 = 3 \text{ s}^{-1}$, (iv) $\dot{\lambda}_1 = 4 \text{ s}^{-1}$.

observed for large values of stretch rates since T_m is much smaller than T_v . The results for these calculations are shown in Figs. 8 and 9 for $\lambda_1 = 2$ as the value of the maximum obtained stretch. As observed from Fig. 8, starting at $t = 0$, the magnetic field first falls and then rises due to an increase in λ_1 . As λ_1 reduces, h_1 comes down approaching a steady equilibrium value. High values of q_v and r_v cause a high initial magnetic field and a faster approach towards the equilibrium.

Dependence of this process on the applied magnetic induction and the stretch rate is shown in Fig. 9. The different start and end points of the curves in Fig. 9a correspond to the values of magnetic field caused by different magnetic inductions. A higher magnetic induction causes a larger magnetic field while for a lower value of stretch rate, as observed from Fig. 9b, the magnetic field approaches the steady equilibrium value earlier in the cycle.

4.4 Time dependent magnetic induction

In this case we study the effect of a time-varying magnetic induction on the induced stress and magnetic field in an undeformed material. The sample is assumed to be fixed at zero deformation and a magnetic induction is applied at time $t = 0$ in the x_1 direction with a constant rate until a value of $B_1 = 0.8$

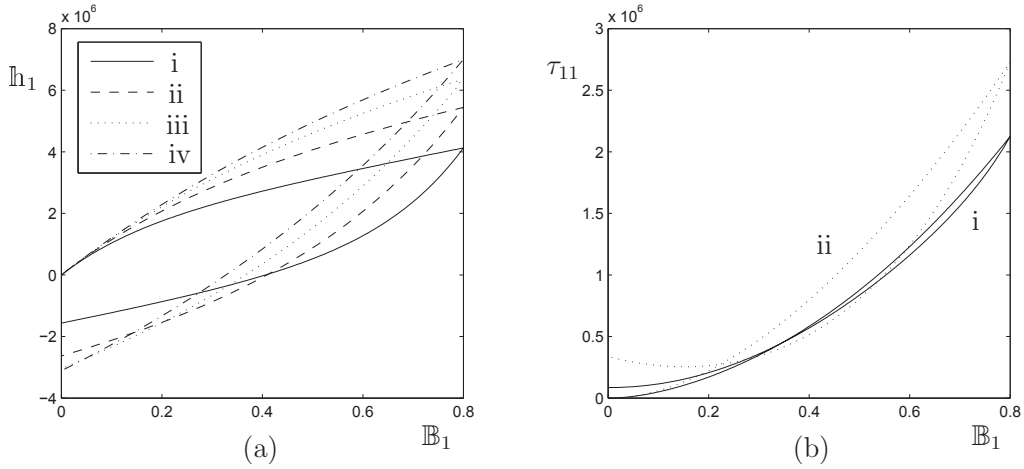


Fig. 10. Time dependent magnetic induction, variation with the rate of magnetic induction **(a)** Total magnetic field h_1 (A/m) vs magnetic induction B_1 (T) (i) $\dot{B}_1 = 1$ T/s, (ii) $\dot{B}_1 = 2$ T/s, (iii) $\dot{B}_1 = 3$ T/s, (iv) $\dot{B}_1 = 4$ T/s; **(b)** Principal total cauchy stress τ_{11} (N/m²) vs magnetic induction B_1 (T). (i) $\dot{B}_1 = 1$ T/s, (ii) $\dot{B}_1 = 4$ T/s.

T is obtained. The induction is then reduced with the same rate until it reaches zero. Numerical results for this case are shown in Figs. 10–13. A value of $\dot{B}_1 = 2$ T/s is used to plot the curves in Figs. 11–13.

It is observed from Fig. 10a that for a particular value of induction rate, the magnetic field increases with an increasing magnetic induction and in the return cycle, it reduces to eventually obtain a negative value. In the entire cycle, the material develops a magnetisation in the x_1 direction due to the existing magnetic induction. As the induction reduces to zero, the material has to develop a magnetic field in the negative x_1 direction to erase the magnetisation in x_1 direction. Also, it can be seen by Eq. (4) that if $\mathfrak{b} = \mathbf{0}$, then \mathfrak{h} and \mathfrak{m} obtain opposite signs.

A higher rate of magnetic induction causes the magnetic field to reach a high peak value and it also causes the magnetic field to reach the maximum negative value when B vanishes completely. Stress in this case has a rather interesting variation as observed from Fig. 10b. Starting from zero, the stress increases with an increasing B_1 and then falls as B_1 is reduced to zero. However, for a high induction rate of $\dot{B}_1 = 4$ T/s, in the return cycle the stress approaches a minimum and then rises again.

A larger value of q_v causes a higher value of peak magnetic field and a larger negative value at the end of cycle as $B_1 \rightarrow 0$. Moreover, it also

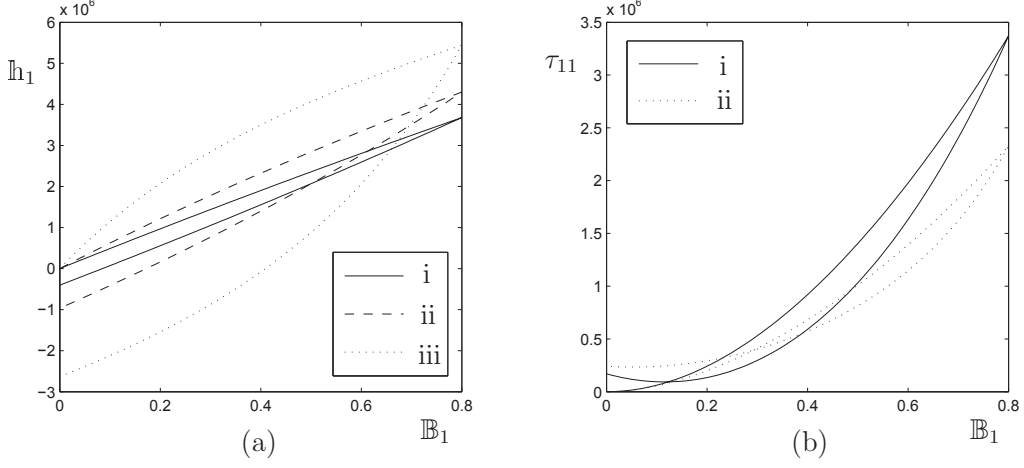


Fig. 11. Time dependent magnetic induction, variation with the parameter q_v **(a)** Total magnetic field h_1 (A/m) vs magnetic induction B_1 (T) (i) $q_v = 0.1/\mu_0$, (ii) $q_v = 1/\mu_0$, (iii) $q_v = 5/\mu_0$; **(b)** Principal total cauchy stress τ_{11} (N/m²) vs magnetic induction B_1 (T). (i) $q_v = 0.1/\mu_0$, (ii) $q_v = 5/\mu_0$.

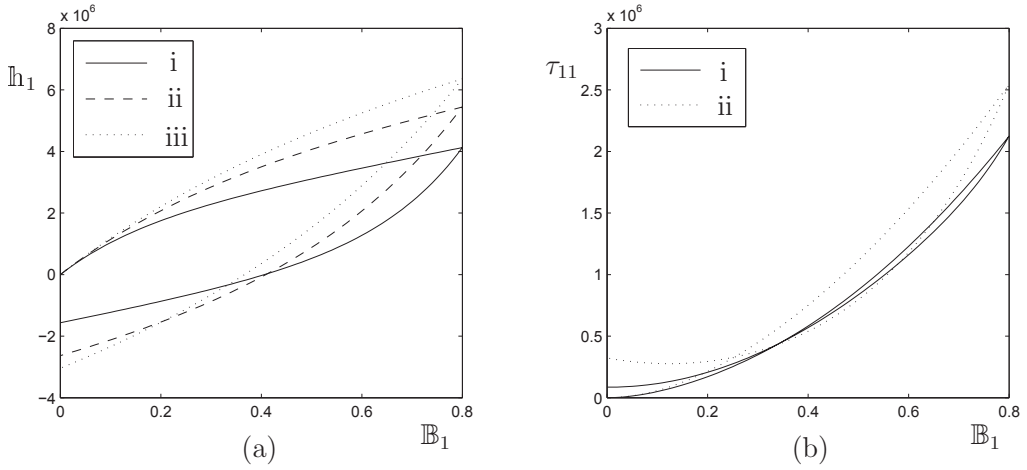


Fig. 12. Time dependent magnetic induction, variation with the specific relaxation time T_m **(a)** Total magnetic field h_1 (A/m) vs magnetic induction B_1 (T) (i) $T_m = 1$ s, (ii) $T_m = 2$ s, (iii) $T_m = 3$ s; **(b)** Principal total cauchy stress τ_{11} (N/m²) vs magnetic induction B_1 (T). (i) $T_m = 1$ s, (ii) $T_m = 3$ s.

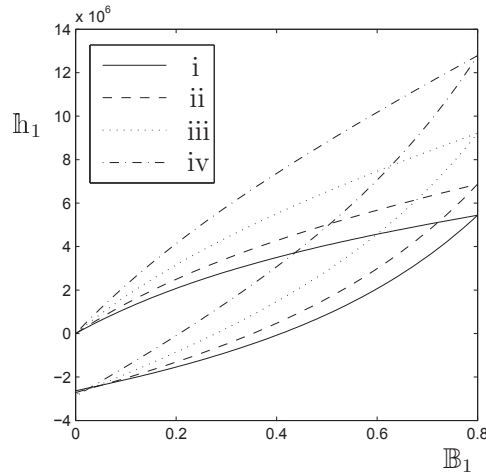


Fig. 13. Variation of the total magnetic field h_1 (A/m) with the magnetic induction B_1 (T), $\dot{B}_1 = 2$ T/s, (i) $\lambda_1 = 1$, (ii) $\lambda_1 = 1.2$, (iii) $\lambda_1 = 1.4$, (iv) $\lambda_1 = 1.6$.

clearly causes larger energy dissipation during the cycle as the area inside the curve (iii) of Fig. 11a is much larger than that in curve (i). The stress in Fig. 11b has a higher peak value for a smaller value of q_v while a larger value of q_v causes a higher stress at the end of the cycle. A smaller value of the parameter T_m helps the material to relax in lesser amount of time, hence the peak values of the magnetic field and stress reached in Fig. 12 in this case are lower. A higher stretch in Fig. 13 causes a larger peak value of the magnetic field.

5 Concluding remarks

We have presented a theory to model nonlinear magneto-viscoelastic deformations in this paper. The deformation gradient is multiplicatively decomposed and the magnetic induction is additively decomposed to ‘elastic’ and ‘viscous’ parts to take into account dissipation mechanisms. A Mooney–Rivlin type magnetoelastic energy density function is used for the equilibrium part, which is simplified to a neo-Hookean type energy density function for the non-equilibrium part of the free energy. These, along with thermodynamically consistent evolution laws, are used to obtain numerical solutions corresponding to several different magneto-viscoelastic deformations.

The magneto-viscoelastic parameters q_v and r_v can have strong effects on

the non-equilibrium magnetic field and the non-equilibrium total Cauchy stress by changing their peak values and the decay times. Strong couplings are also shown to exist between the magnetic induction and the non-equilibrium stress, and the underlying deformation and the non-equilibrium magnetic field, as is evident from Figs. 4b and 6a. We observe that a stretch rate and a magnetic induction rate can have a considerable influence on the total Cauchy stress and the magnetic field. The developed model seems to capture the magneto-viscoelastic phenomena quite nicely and on isolating mechanical viscoelastic effects, our results are qualitatively the same as those obtained earlier by Amin et al. (2006) and Hossain et al. (2012).

It should be noted that the numerical results presented here are representative solutions considering only one dissipation mechanism in the body. The theory can be easily generalised to include multiple mechanisms to match the experimental data. We have considered a specific type of phenomenologically motivated constitutive law for an isotropic material in this paper. The theory for an anisotropic material and possibility of existence of other constitutive laws (such as those derived from micromechanics of the material) will be discussed in forthcoming contributions.

Acknowledgements:

This work is funded by an ERC advanced grant within the project MO-COPOLY.

References

- Amin, A.F.M.S., Lion, A., Sekita, S., Okui, Y., 2006. Nonlinear dependence of viscosity in modeling the rate-dependent response of natural and high damping rubbers in compression and shear: Experimental identification and numerical verification. *Int. J. Plast.* 22, 1610–1657.
- Bergström, J. S., Boyce, M. C., 1998. Constitutive modeling of the large strain time-dependent behavior of elastomers. *J. Mech. Phys. Solids.* 46, 931–954.
- Bird, R., Curtiss, C. F., Armstrong, R. C., Hassager, O., 1987. *Dynamics of Polymeric Liquids, Kinetic Theory*. Wiley, New York, USA.
- Boczkowska, A., Awietjan, S. F., 2009. Smart composites of urethane elastomers with carbonyl iron. *J. Mater. Sci.* 44, 4104–4111.

- Böse, H., Rabindranath, R., Ehrlich, J., 2012. Soft magnetorheological elastomers as new actuators for valves. *J. Intell. Mater. Syst. Struct.* 23, 989–994.
- Böse, H., Röder, R., 2009. Magnetorheological elastomers with high variability of their mechanical properties. *J. Phys.: Conf. Ser.* 149, 012090.
- Bustamante, R., Dorfmann, A., Ogden, R. W., 2007. A nonlinear magnetoelastic tube under extension and inflation in an axial magnetic field: numerical solution. *J. Eng. Math.* 59, 139–153.
- Coleman, B. D., Noll, W., 1963. The thermodynamics of elastic materials with heat conduction and viscosity. *Arch. Ration. Mech. Anal.* 13, 167–178.
- de Gennes, P. G., 1971. Reptation of a polymer chain in the presence of fixed obstacles. *J. Chem. Phys.* 55, 572–579.
- Doi, M., Edwards, S. F., 1988. *The Theory of Polymer Dynamics*. Clarendon press, Oxford.
- Dorfmann, A., Ogden, R. W., 2003. Magnetoelastic modelling of elastomers. *Eur. J. Mech. A/Solids*. 22, 497–507.
- Dorfmann, A., Ogden, R. W., 2004. Nonlinear magnetoelastic deformations. *Q. J. Mech. Appl. Math.* 57, 599–622.
- Eringen, A. C., Maugin, G. A., 1990. *Electrodynamics of Continua*, vol. 1. Springer-Verlag.
- Ginder, J. M., Clark, S. M., Schlotter, W. F., Nichols, M. E., 2002. Magnetostrictive phenomena in magnetorheological elastomers. *Int. J. Mod. Phys. B*. 16, 2412–2418.
- Green, M. S., Tobolsky, A. V., 1946. A New Approach to the Theory of Relaxing Polymeric Media. *J. Chem. Phys.* 14, 80–92.
- Holzappel, G. A., Simo, J. C., 1996. A new viscoelastic constitutive model for continuous media at finite thermomechanical changes. *Int. J. Solids Struct.* 33, 3019–3034.
- Hossain, M., Vu, D. K., Steinmann, P., 2012. Experimental study and numerical modelling of VHB 4910 polymer. *Comput. Mater. Sci.* 59, 65–74.

- Huber, N., Tsakmakis, C., 2000. Finite deformation viscoelasticity laws. *Mech. Mater.* 32, 1–18.
- Jolly, M. R., Carlson, J. D., Muñoz, B. C., 1996. A model of the behaviour of magnetorheological materials. *Smart Mater. Struct.* 5, 607–614.
- Kaliske, M., Rothert, H., 1997. Formulation and implementation of three-dimensional viscoelasticity at small and finite strains. *Comput. Mech.* 19, 228–239.
- Koprowski-Theiss, N., Johlitz, M., Diebels, S., 2011. Characterizing the time dependence of filled EPDM. *Rubber Chem. Tech.* 84, 147–165.
- Linder, C., Tkachuk, M., Miehe, C., 2011. A micromechanically motivated diffusion-based transient network model and its incorporation into finite rubber viscoelasticity. *J. Mech. Phys. Solids.* 59, 2134–2156.
- Lion, A., 1997. A physically based method to represent the thermo-mechanical behaviour of elastomers. *Acta Mech.* 123, 1–25.
- Lubliner, J., 1985. A model of rubber viscoelasticity. *Mech. Res. Commun.* 12, 93–99.
- Miehe, C., Göktepe, S., 2005. A micro-macro approach to rubber-like materials. Part II: The micro-sphere model of finite rubber viscoelasticity. *J. Mech. Phys. Solids.* 53, 2231–2258.
- Otténio, M., Destrade, M., Ogden, R. W., 2008. Incremental magnetoelastic deformations, with application to surface instability. *J. Elast.* 90, 19–42.
- Pao, Y. H., 1978. Electromagnetic forces in deformable continua, in: Nemat-Nasser, S. (Ed.), *Mechanics Today*, vol. 4, Oxford University Press, pp. 209–305.
- Reese, S., 2003. A micromechanically motivated material model for the thermo-viscoelastic material behaviour of rubber-like polymers. *Int. J. Plast.* 19, 909–940.
- Reese, S., Govindjee, S., 1998. A theory of finite viscoelasticity and numerical aspects. *Int. J. Solids Struct.* 35, 3455–3482.
- Saxena, P., Ogden, R. W., 2011. On surface waves in a finitely deformed magnetoelastic half-space. *Int. J. Appl. Mech.* 3, 633–665.

- Shampine, L. F., Reichelt, M. W., 1997. The MATLAB ODE suite. *SIAM J. Sci. Comput.* 18, 1–22.
- Simo, J.C., 1987. On a fully three-dimensional finite-strain viscoelastic damage model: Formulation and computational aspects. *Comput. Methods Appl. Mech. Eng.* 60, 153–173.
- Varga, Z., Filipcsei, G., Zrínyi, M., 2006. Magnetic field sensitive functional elastomers with tuneable elastic modulus. *Polymer*, 47, 227–233.